Airborne observations for verification of the GHG emission estimates.

Shamil Maksyutov, Rajesh Janardanan, Fenjuan Wang, Lorna Nayagam, Tsuneo Matsunaga.

National Institute for Environmental Studies, Tsukuba, Japan

Short comment on validation of area fluxes

- Comparison of methane inversions with airborne observations
  - Comparing prior and posterior simulated CH4 with airborne observations over India by Janardanan et al (2020), and Australia (Wang et al, 2025)

CEOS AC-VC, 13 June, Takamatsu, Kagawa, Japan

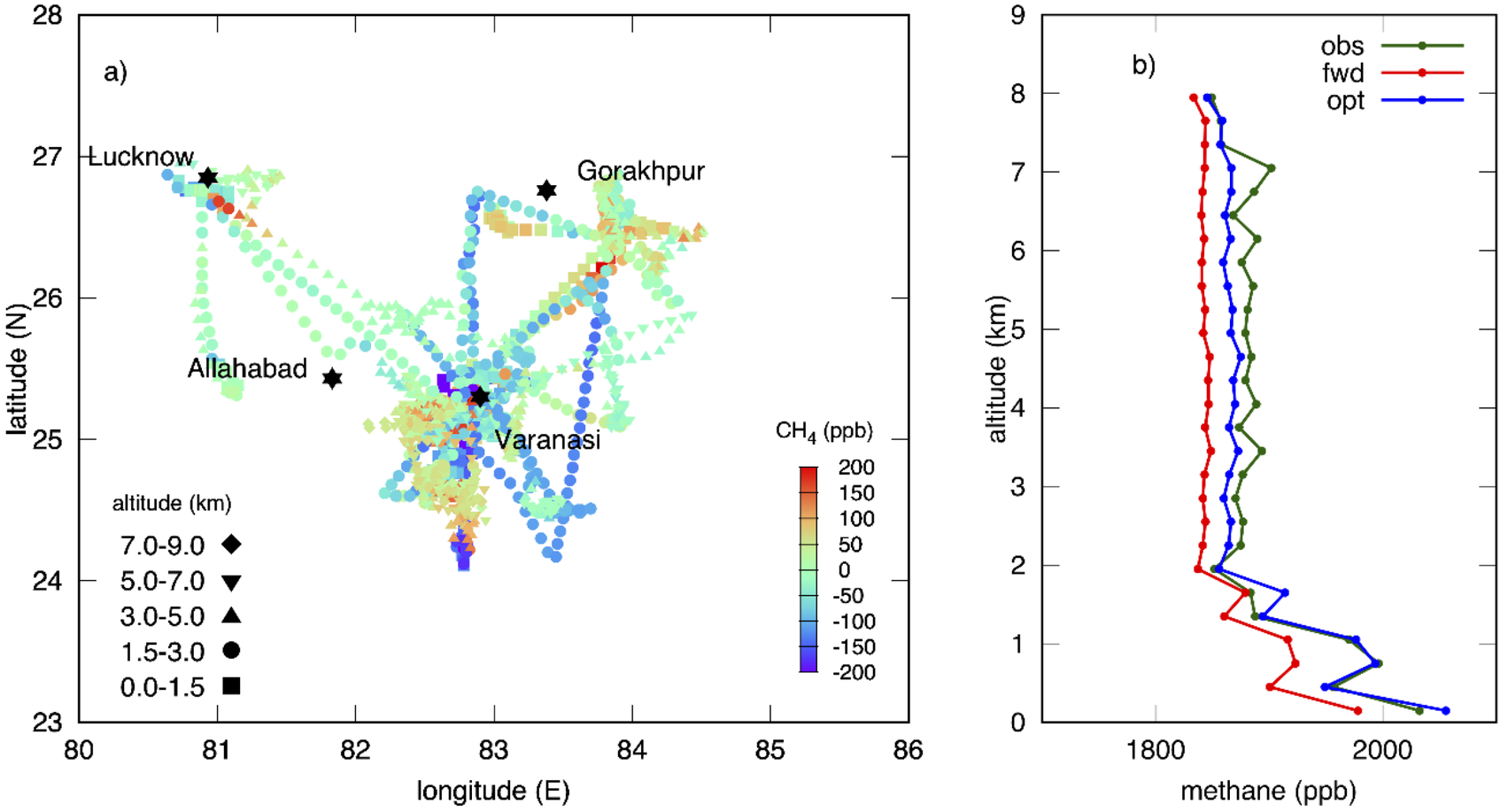

Janardanan et al Remote Sensing 2020
https://doi.org/10.3390/rs12030375

Figure 5. (a) Track of aircraft observation of methane over the Indian domain, where the colors show the difference between optimized forward and observations. To facilitate visual clarity, not all observations are shown. The black stars represent cities around the region. Names of the cities are labeled in black. Observations at different altitudes are shown with different symbols, as shown in the legend. (b) The vertical profile of 300 m - averaged all aircraft observations against prior forward and optimized forward simulations. Red- prior, blue – optimized w inversion

Inverse model results over India compared to airborne observations, show improved fit after inversion.

Table 1. List of countries with annual emission (natural or anthropogenic) greater than 2.5 Tg CH_4. Annual prior and posterior emission for total, natural, and anthropogenic categories and their percentage difference after optimization are given. The final row corresponds to global values. Country codes are listed against country names in the appendix, Table A2.

Country Code	Total Prior	Total Posterior	Percentage Difference	Natural Prior	Natural Posterior	Percentage Difference	Anthropogenic Prior	Anthropogenic Posterior	Percentage Difference	Posterior-Prior (Anthropogenic)	Uncertainty (Tg)
CHN	60.1	52.0	−13.5	5.8	6.3	7.7	54.3	45.7	−15.8	−8.6	8.6
USA	51.6	55.7	7.9	23.8	25.9	8.8	27.8	29.8	7.2	2.0	7.8
RUS	47.8	45.2	−5.5	13.6	13.2	−2.7	34.2	31.9	−6.6	−2.3	7.8
BRA	45.6	56.2	23.3	29.2	39.8	36.1	16.4	16.5	0.6	0.1	10.0
IND	29.9	36.5	21.9	9.9	12.3	25.2	20.1	24.2	20.4	4.1	5.3
CAN	23.4	16.4	−29.8	19.7	12.2	−37.8	3.7	4.2	12.4	0.5	4.5

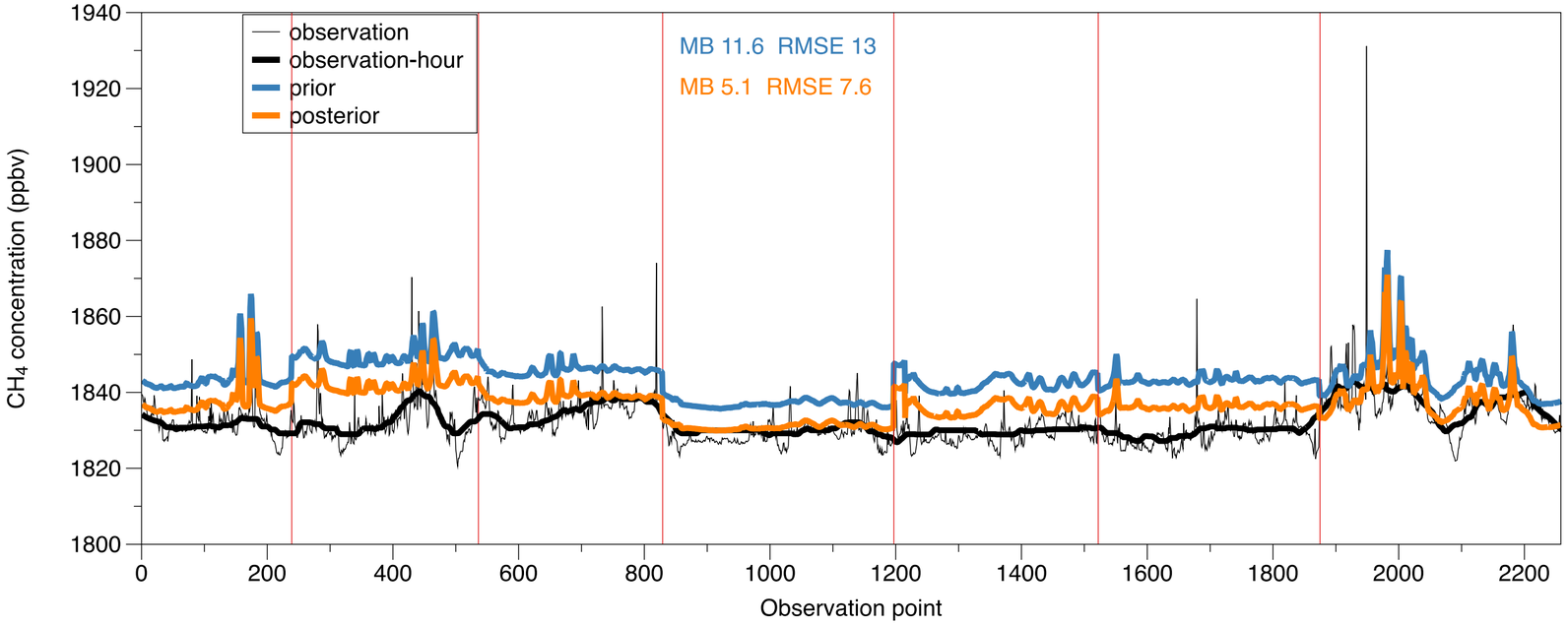

Wang et al, GIS Sci RS 2025
https://doi.org/10.1080/15481603.2025.2488595

Figure 5. ARA 2018 airborne observations and modeled CH_4 discrepancies driven by prior and posterior fluxes. The bold black line represents the hourly moving average of the observations. The mean bias (MB) and root-mean-square error (RMSE) are also shown in ppbv. The red lines separate observation dates during September 10 to 21.

Comparison to airborne observations show that large emissions plumes are captured by inversion.

Table 1 Comparison of anthropogenic emissions in Australia (2016-2021).

(Kt CH_4 yr^{-1})	UNFCCC	EDGARv8.0 (Crippa et al., 2023)	EDGARv7.0	prior	posterior
Average	4639	4408	4443	4239	4198
Standard deviation	192	145	112	106	79